

Control of the hydrogen:deuterium isotope mixture using pellets in JET

Original

Control of the hydrogen:deuterium isotope mixture using pellets in JET / Valovi, M.; Baranov, Y.; Boboc, A.; Buchanan, J.; Citrin, J.; Delabie, E.; Frassinetti, L.; Fontdecaba, J. M.; Garzotti, L.; Giroud, C.; Mckean, R.; Lerche, E.; Kiptily, V.; Köchl, F.; Marin, M.; Maslov, M.; Menmuir, S.; Tvalashvili, G.; Weisen, H.; Subba, F.. - In: NUCLEAR FUSION. - ISSN 0029-5515. - 59:10(2019). [10.1088/1741-4326/ab3812]

Availability:

This version is available at: 11583/2986800 since: 2024-03-11T14:54:42Z

Publisher:

IOP PUBLISHING LTD

Published

DOI:10.1088/1741-4326/ab3812

Terms of use:

This article is made available under terms and conditions as specified in the corresponding bibliographic description in the repository

Publisher copyright

IOP preprint/submitted version

This is the version of the article before peer review or editing, as submitted by an author to NUCLEAR FUSION. IOP Publishing Ltd is not responsible for any errors or omissions in this version of the manuscript or any version derived from it. The Version of Record is available online at <https://dx.doi.org/10.1088/1741-4326/ab3812>.

(Article begins on next page)

Control of H:D isotope mixture with pellets in JET

M Valovič¹, Y Baranov¹, G Buchanan¹, J Citrin², E Delabie³, L Frassinetti⁴, J M Fontdecaba⁵, L Garzotti¹, C Giroud¹, R McKean¹, E Lerche^{1,6}, V Kiptily¹, F Köchl^{1,7}, M Marin², M Maslov¹, S Menmuir¹, G Tvalashvili¹, H Weisen¹ and the JET Contributors⁸

EUROfusion Consortium, JET, Culham Science Centre, Abingdon, OX14 3DB, UK

¹*CCFE, Culham Science Centre, Abingdon, OX14 3DB, UK*

²*DIFFER P.O. Box 6336, 5600 HH Eindhoven, The Netherlands*

³*Oak Ridge National Laboratory, Oak Ridge, Tennessee, United States of America*

⁴*KTH Royal Institute of Technology, TEKNIKRINGEN 31, Sweden*

⁵*Laboratorio Nacional de Fusión, Ciemat, 28040 Madrid, Spain*

⁶*LPP-ERM/KMS, Association EUROFUSION-Belgian State, TEC partner, Brussels, Belgium*

⁷*Fusion@ÖAW, Atominstitut, TU Wien, Stadionallee 2, A-1020 Vienna, Austria.*

⁸*See the author list of “Overview of the JET preparation for Deuterium-Tritium Operation” by E. Joffrin et al. to be published in Nuclear Fusion Special issue: overview and summary reports from the 27th Fusion Energy Conference (Ahmedabad, India, 22-27 October 2018)*

E-mail: martin.valovic@ukaea.uk

Abstract. Deuterium pellets are injected into initially pure hydrogen H-mode plasma in order to control H:D isotope mixture. The pellets are deposited in outer 20% of minor radius, similar to that expected in ITER creating transiently hollow electron density profiles. The isotope mixture of H:D ~ 45:55% is obtained in the core with pellet fuelling throughput of $\Phi_{pel} = 0.045 P_{aux}/T_{e,ped}$ similar to previous pellet fuelling experiments in pure deuterium. Evolution of H:D mix in the core is reproduced using simple model although deuterium transport could be higher at the beginning of the pellet train compared to the flat top phase.

1. Introduction

To maximise power produced by a fusion reactor the deuterium-tritium isotope mixture should be kept close to 50:50%. This can be achieved simply by fuelling the reactor by pre-mixed DT fuel. Such fuelling scheme would avoid isotope separation in reactor's outer fuel loop and leaves only the necessity to separate hydrogen isotopes from helium and impurities. Avoiding isotope separation will reduce the cost of the reactor but more importantly it will decrease the dwell time of tritium in the outer loop and reduce the amount of tritium in a reactor.

Removing the isotope separation completely from the fuel loop could however make an isotope mix control impossible. The deuterium – tritium ratio in the plasma core can gradually drift from pre-mixed value due to a number of reasons. Firstly, gyrokinetic analysis and modelling have identified mechanisms for tokamak particle transport coefficient differentiation between hydrogenic isotopes [1, 2, 3, 4], although in practice the resultant density profile separation is expected to be weak; the isotope dependence of pedestal transport is more uncertain however. Secondly, for engineering reasons neutral beams are likely to inject pure deuterium as planned on ITER. Although the fuelling efficiency of neutral beams is low it is still comparable to the fusion rate and thus beams could lead to excess of D

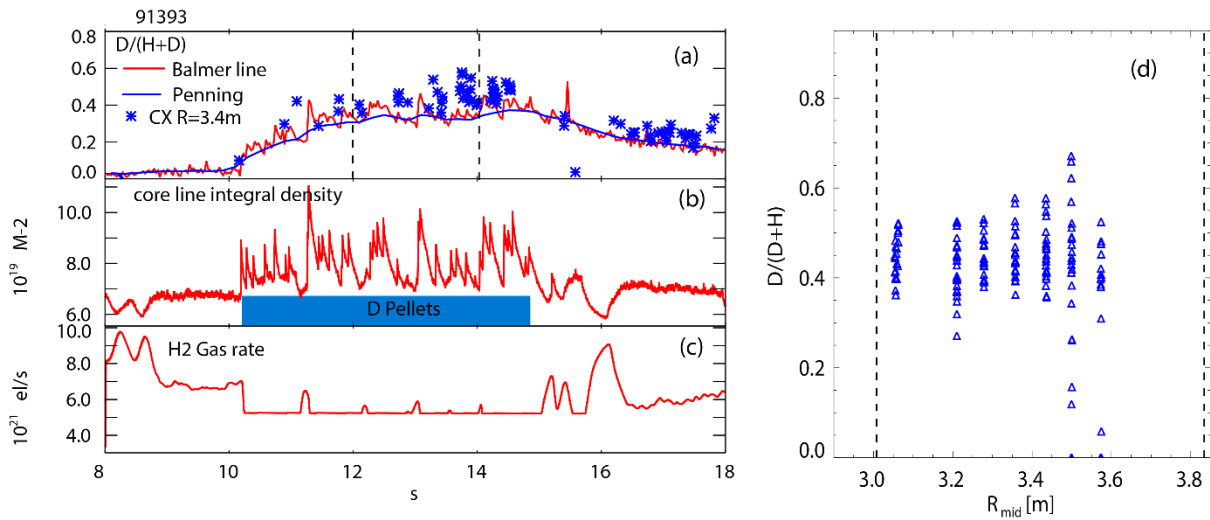


Figure 1. Temporal evolution of relevant parameters during the isotope control experiment. Traces from the top to the bottom: (a) isotope mix ratio from: Balmer line spectroscopy - red line, Penning pressure gauges in divertor - blue line, CX spectroscopy at $R=3.43\text{m}$ – blue symbols, (b) core line integrated density $n_e L$, (c) hydrogen gas puff rate, (d) isotope mix ratio profile from CX spectroscopy for time interval shown by vertical lines on panel (a), vertical lines in panel (d) represent separatrix and magnetic axis respectively. For given radius different data points represent different times.

in plasma core. It could be mentioned here however that in ITG regimes the sensitivity of isotope peaking to isotope source is expected to be weak [4, 5], and depends more on core isotope boundary conditions and the electron density peaking. Finally, the departure from a 50:50% isotope mix can arise from different particle exhaust and wall recycling for deuterium and tritium and impacting the core boundary conditions. Due to all these uncertainties ITER is planning full isotope separation and two sets of pellet injectors, one for pure tritium and one for pure deuterium [6, 7]. In DEMO a compromised solution with partial separation (bypass) is considered [8].

The requirement for accuracy of isotope mix control itself is not very demanding. At fixed electron density, ignoring helium and impurities, keeping fusion power within say 5% of its maximum value requires the deuterium–tritium density ratio within of $n_T/(n_D + n_T) = 0.4 - 0.6$. The main uncertainty is the time scale at which the isotope ratio should be controlled in this window and what throughput of pure tritium is required to achieve that.

This question cannot be answered directly even on JET as the pellet injector is not designed to operate in tritium. Nevertheless, pellet fuelling experiments can be designed in JET which address the aforementioned problem partially. Firstly, deuterium pellets could be injected into plasma which was pre-fuelled by tritium gas and beams, and such an experiment is proposed for the next DT campaign in JET. Another possibility of how to contribute is to inject combinations of hydrogen and deuterium pellets and observe and understand different isotope behaviour. The present paper describes one such experiment in which pure deuterium pellets were injected into hydrogen plasma and successfully

maintained the H:D isotope mix close to the 50:50% target. We note that isotope control using pre-mixed HD pellets was performed on ASDEX Upgrade [9] including very detailed documentations of the preparation and diagnostics of mixed isotope pellets.

2. Experimental setup

The experiment was performed on JET with ITER like walls with plasma current $I_p = 1.4MA$ and toroidal field on geometric axis $B_T = 1.7 T$. The divertor was in corner configuration for both inner and outer leg. Plasma fuelling was provided by hydrogen gas with a rate of $\Phi_{H_2,gas} = 6.7 \times 10^{21} at/s$, which was reduced to $5.2 \times 10^{21} at/s$ during the pellet phase (see figure 1c).

The plasma was heated by hydrogen neutral beams with total flat top power of $P_{NBI} = 6.3MW$. The corresponding particle source from beams is $\Phi_{H_2,NBI} = 1.5 \times 10^{21} at/s$. In addition, RF heating at second harmonic hydrogen resonance ($\omega = 2\omega_{cH}$, 51MHz) is used with total power of $P_{RF} = 3.3MW$ so that the total auxiliary heating power during flattop is $P_{aux} = 9.6MW$.

After stationary hydrogen H-mode is established, additional fuelling by deuterium pellets from the high field side is applied (see figure 1b). Each pellet causes a sharp increase of the line integrated plasma density. The nominal pellet volume given by extruder is $40mm^3$ but by using the ‘‘double cut’’ technique we reduced the pellet volume approximately by a factor of two to get closer to ITER situation. Before pellets are injected into the plasma their frequency and size are measured by microwave cavity utilising the change of resonance in the presence of pellet. The averaged values over the interval $t = 12.2 - 15.0s$ are $f_{pel} = 9.7Hz$ for pellet frequency and $N_{pel} = 8.5 \times 10^{20} at$ for pellet particle contents so that the pellet fuelling rate is $\Phi_{pel} = 8.2 \times 10^{21} at/s$. The pellet velocity is $\sim 90m/s$.

3. Measurement of isotope mix ratio

During pellet injection of deuterium pellets into hydrogen plasma the isotope mix ratio was measured by four independent methods as listed below.

3.1 From neutrals

Figure 1a shows the ratio $n_D/(n_H + n_D)$ as measured by Balmer-alpha spectroscopy in the divertor and in the Penning gauges in the subdivertor. The values agree well which is not surprising as both methods measure isotope mix ratio of neutrals in the divertor region. It can be also observed that both ratios need about 2 seconds to reach the flattop value of:

$$n_D/(n_H + n_D)_{edge\ neutrals} \approx 0.35.$$

3.2 From CX

The Charge Exchange (CX) spectroscopy signal measures the isotope ratio of ions in the plasma core. The method fits two Gaussian functions to the hydrogen and deuterium Balmer lines assuming the same

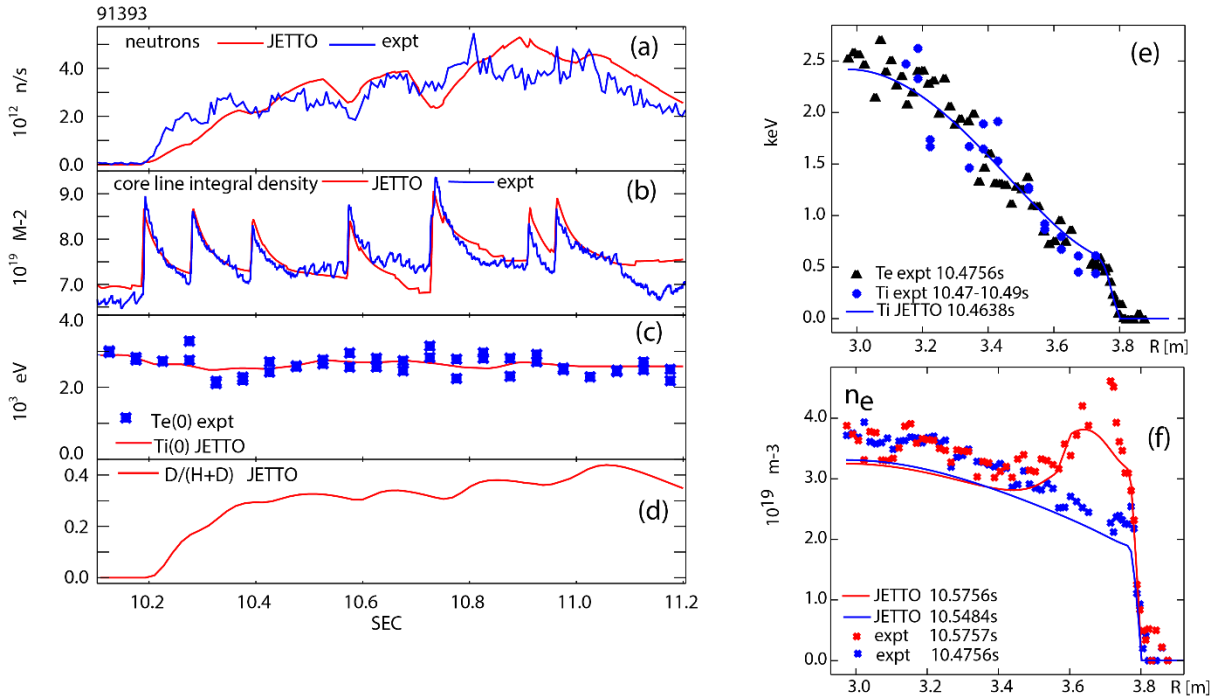


Figure 2. Simulation of isotope mix by JETTO code. (a) total neutron rate $R_{DD,th}$, (b) core line integrated density $n_e L$, (c) central electron temperature from Thomson scattering (blue + symbols) and central ion temperature as imported into JETTO (red line), (d) calculated central isotope mix ratio $n_D/(n_H + n_D)$ from neutron rate, (e) electron and ion temperatures and (f) electron density profiles before and after 4th pellet. In panels (e) and (f) electron density and temperature is measured by Thomson scattering.

temperature for both isotopes. The key element of the fit is a subtraction of passive background light using beam modulation and subtraction of passive frames without ELMs or pellets during the exposure time from similar frames during the beam on time. The details of this diagnostics will be published elsewhere. In our case the isotope mix ratio can be evaluated well inside the plasma with some limitation close to magnetic axis and outer part of the plasma where error bars become very large. The CX method gives the flattop value of (figure 1a, 1d):

$$n_D/(n_H + n_D)_{R=3.1-3.4m} \approx 0.45.$$

This core value is somewhat higher than the neutral gas measurements from the edge plasma.

3.3 From neutrons

The isotope mix ratio can be deduced indirectly from a neutron rate. Figure 2a shows that application of deuterium pellets causes an increase of neutron rate from virtually zero to the flat top value of $R_n = (3-4) \times 10^{12}$ 1/s, confirming that the deuterium from pellets penetrated into the plasma core and produced DD fusion reactions. Assuming that all neutrons are the result of a thermal DD reaction and knowing the density and temperature profiles one can convert the neutron rate into the isotope mix ratio in the centre. The problem is the discrete nature of pellet fuelling which makes the plasma density

transient at all times. To include this element into the analysis, we calculated the plasma density by a model while keeping the temperature fixed from the measurement. The model evolves independently hydrogen and deuterium densities as a response to particle sources and particle transport. In other words temperature is treated interpretatively while densities are treated predictively. The simulation was done by JINTRAC code suite [10]. The particle sources include beams, pellets and neutrals, and are calculated by PENCIL, HPI2 and FRANTIC codes respectively. The boundary condition for FRANTIC is set by neutral hydrogen flux Φ_0 at separatrix.

The particle transport is modelled by JETTO code. For plasma core the particle diffusivity is used as $D = C_D \times \chi_{BgB}$, where χ_{BgB} is the geometric average of electron and ion Bohm/gyro-Bohm heat diffusivities [10, 11] and the C_D multiplier is set the same for hydrogen and deuterium. In addition, modest inward anomalous pinch is included as: $v/D = -C_V r/a^2$. This core particle transport modelling is interpretive in nature and the motivation of this was to infer the D and V particle transport coefficients leading to experimental agreement, for later comparison with higher-fidelity first-principle-based modelling. At the plasma edge the particle transport is modelled by “continuous ELM model” [12] in which the particle diffusivity inside edge transport barrier is enhanced when the pressure gradient exceeds a critical value: $\alpha > \alpha_{crit}$. Comparison of simulation of edge density with experimental data reveals that the aforementioned ELM model does not describe fully the post pellet ELM loss mechanism. Namely ELMs remove pellet material faster than in the model and they also act deeper than edge transport barrier. To include this we added transient post pellet outward convection in the form of $v = v_0 \times \exp\{-(t - t_{pel})/\tau + (r/a - 1)/\Delta\}$ where v_0 is the amplitude of outward convection, τ is the duration of the enhanced post pellet convection and Δ is the normalised radial depth of the zone of the enhanced convection. Note that the need to enhance the radial extent of ELM related particle losses deeper than the pedestal width has been recognised in previous simulations [13].

Figure 2 shows the result of the simulation with the following parameters $\Phi_0 = 2.7 \times 10^{21} \text{at/s}$, $C_D = 4.5$, $C_V = 0.4$, $v_0 = 7 \text{m/s}$, $\tau = 50 \text{ms}$, $\Delta = 0.25$, and using the same values for hydrogen and deuterium. The calculation is performed in a limited time interval starting just before the first pellet and finishing after the 7th pellet i.e. when approximately the neutron rate reaches its maximum value.

Figures 2c, 2e and 2f document how the experimental ion temperature was imported into the simulation, in particular its central value on which the thermal DD fusion rate is very sensitive. The central ion temperature from carbon and neon charge exchange is measured with coarse time resolution and with a larger error bar. Nevertheless, in our plasma the electron and ion temperature are similar with good accuracy as seen in panels 2e and 2f and we assume $T_i = T_e$. In addition, figure 2c shows that the central electron temperature is quite constant in time without transients which would otherwise introduce large variation of neutron rate.

Figures 2b and 2f compare measured and calculated electron density. It is seen that the simulations reproduce well temporal evolution of line integrated electron density including pellet induced transients.

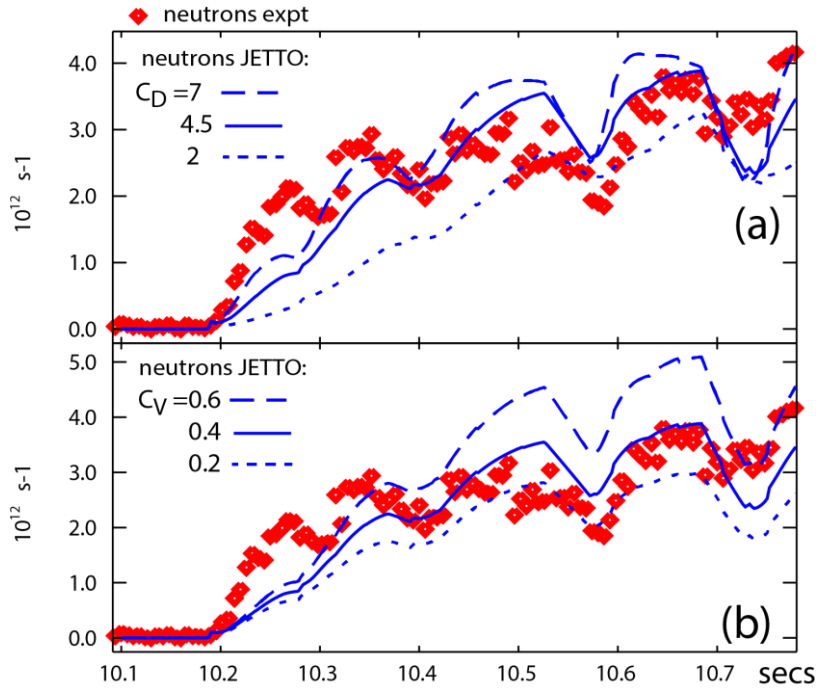


Figure 3. Comparison of measured and simulated neutron rate during the scan of particle transport coefficients: (a) diffusivity scan with $C_D = 2, 4.5, 7$ at $C_V = 0.4$. (b) pinch velocity scan with $C_V = 0.2, 0.4, 0.6$ at $C_D = 4.5$

The comparison of density profiles across the 4th pellet (fig. 2f) also shows that density peaking just before pellet is well captured by simulation. The model also describes the pellet deposition depth as calculated by HPI2 module [14] and confirms the shallow pellet deposition, similar to that expected in ITER. The simulation sometimes underestimates the amplitude of the pellet density perturbation. This is a result of continuous ELM model which starts to remove the pellet particles already during the pellet deposition phase. This is in contrast with an experiment where pellet particles are removed in discrete steps during the ELMs as described in the next section.

Figure 2a compares the measured neutron rate with that calculated by JETTO code. The neutron rate was also checked with TRANSP [15] and good agreement with JETTO was found. The agreement between measured and calculated neutron rate by JETTO is rather good taking into account the large sensitivity of thermal DD reaction rate on ion temperature. The simulation also describes well the transient responses of neutron rate on individual pellets during the flat top phase. The sensitivity of calculated neutron rate to a selection of transport parameters is illustrated in scans shown in figure 3. It is seen that the experimental neutron rate can be broadly bracketed by simulations using diffusivity parameters $C_D = 2 - 7$ and $C_V = 0.2 - 0.6$. The wide range of these parameters does not mean that they represent the uncertainty in the fit. They rather reflect the fact that these parameters vary in time while in our simulations they are constant. This is clearly seen in figure 3 by comparing the neutron rate during 1st and 4th pellet (at 10.2s and 10.6s respectively). At 4th pellet the choice $C_D = 4.5$ and $C_V = 0.4$

fits well with the neutron rate while the same setting at the 1st pellet systematically underestimates the measured neutron rate.

We do not have full explanation for this discrepancy. One possibility is the isotope dependence of particle diffusivity. During the first pellet, plasma is still predominantly composed of hydrogen while during the 4th pellet about 1/3 of ions is deuterium so that the effective ion diffusivity could be higher at the beginning of pellet train compared to later phases. Another possible explanation is the increase of neutron rate due to a non-Maxwellian distribution of deuterium ions. Indeed, inspection of neutral particle analyser spectra show an increase of deuteron fluxes in energies 300keV - 800keV with e-folding energy scale 123keV. This increase correlates with the timing of pellet train. There are two possibilities how deuterons can be accelerated to such high energies and both are related to RF heating which is continuously applied before and during the pellet train. The first possible acceleration channel is the parasitic four harmonic resonance $\omega = 4\omega_{cD}$. To test this we ran a shot JPN 91238 with modulated RF heating and found that the changes in neutron rate were fully in line with changes in electron temperature and parasitic resonance was not required to explain neutron rate (note that this shot had deuterium beams so the neutron rate was due to beam-thermal interaction). The second possibility how to accelerate deuterons to aforementioned energies are the elastic nuclear collisions between RF accelerated hydrogen ions with cold deuterium ions, so called knock-on effect. Order of magnitude estimates indicate that such mechanism could produce a neutron rate comparable to the thermal-thermal levels, in particular at the start of pellet train [16]. However even if this mechanism is significant it still requires that deuterons from pellets already propagated to the plasma core, only their density would be lower to accommodate nonthermal neutrons. Regarding the precise quantification of this effect just note that the CX measurements of the isotope mix (see figure 1d) does not show significant reduction of density of deuterium ions towards the plasma core but we do not have the tools needed to evaluate this knock-on effect with accuracy. On the basis of experimental evidence we conclude that the knock-on effect could play a role at the beginning of the pellet train but during the later phase the neutrals are mainly due to thermal DD reactions. Using this assumption figure 2d shows the isotope mix ratio as calculated by the code. At the time of maximum neutron rate (~11s) the ratio is:

$$n_D/(n_H + n_D)_{r=0,neutrons} \approx 0.44.$$

This value is close to the CX measurement and close to the target value of 0.5.

4. Fuelling efficiency

Efficiency of isotope mix control depends on two mechanisms: (1) Amount of pellet particle flux required to keep the plasma density and isotope mix at the plasma edge to the prescribed value and (2) characteristic time of propagation of the isotope mix from pellet deposition zone to plasma core. These two processes contribute to the pellet fuelling efficiency multiplicatively i.e. good efficiency requires

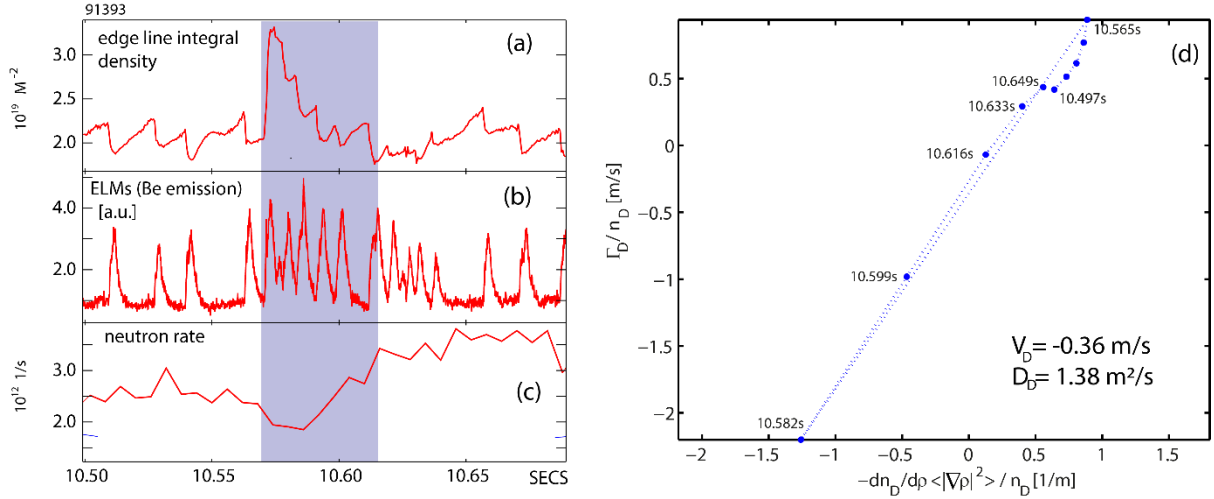


Figure 4. Detail of transient around the 4th pellet. (a) edge line integral density, (b) ELMs signals, (c) neutron rate. Shaded area in panels (a)-(c) approximately represents the interval with inverted density gradient. (d) plot of the normalised particle flux Γ_D/n_D versus normalised density gradient $dn_D/dr/n_D$ at $r/a = 0.5$. corresponding time labels are shown.

simultaneously long enough lifetime of pellet density perturbation and fast enough particle transport in the core. Next sections quantify these two factors separately.

4.1 Pellet particle flux

As shown in previous sections the deuterium pellet particle flux of $\Phi_{pel} = 8.2 \times 10^{21} \text{ at/s}$ is sufficient to keep the isotope mix ratio at $n_D/(n_H + n_D) = 0.45$. At the same time interval the averaged pedestal electron temperature is $T_{e,ped} = 0.33 \pm 0.05 \text{ keV}$ which gives for the pellet fuelling flux of: $\Phi_{pel} = 0.045 P_{aux}/T_{e,ped}$. To compare this value with the case of deuterium pellets and deuterium plasma we can write $\Phi_{pel,D \rightarrow D} = \Phi_{pel} \times (n_H + n_D)/n_D$ which gives:

$$\Phi_{pel,D \rightarrow D} = 0.10 P_{aux}/T_{e,ped}. \quad (1)$$

The front coefficient in eq. (1) is very close to the value of 0.073 found in our previous pellet fuelling experiments in pure deuterium plasmas [17, 18]. This indicates similarity of pellet particle loss mechanism, namely the dominant role of ELMs. Indeed, looking closely at the post pellet line integrated density signal (figure 4a) it is clear that the particles are lost in discrete events coinciding with ELMs. It takes about five ELMs to remove material deposited by a single pellet. This ratio is about the same as expected on ITER where the ELMs/pellet frequency ratio is expected to be about 40Hz/10Hz. Nevertheless the relative pellet size and consequently the ELMs size is larger than permitted on ITER. This is even true for burst of high frequency ELMs which immediately follow the pellet as seen in figure 4. For those ELMs the normalised inverse frequency is $1/(f_{ELMs}\tau_E) = 1/(133\text{Hz} \times 0.13\text{s}) = 5.7\%$

that is about 10 times larger than the value required in ITER. Here $\delta W_{ELM}/W_{tot} = 1/(f_{ELMs}\tau_E)$ is the size of an ELM that would carry all the energy transport losses. In summary the relation (1) is derived under condition of ITER like ratio of ELMs/pellet frequency, but relative sizes of both pellets and ELMs are larger.

4.2 Core particle transport

When pellet is injected into plasma it creates transiently a zone of reversed gradient of deuterium density. As a consequence, the deuterium ion particle flux reverses from outwards to inwards and consequently deuterium concentration in the core increases as manifested by increase of neutron rate signal in figure 4c. This situation is transient. This is detailed in figure 4d where simulated deuterium particle flux at $r/a=0.5$ is plotted against the density gradient during one pellet cycle around 4th pellet. The slope of this graph determines the deuterium particle diffusivity. When evaluated during the post-pellet phase lasting 70ms the linear regression gives $D_D = 1.38m^2/s$ or in normalised units $D_D/\chi_{eff} = 0.41$. Here $\chi_{eff} = q/(n_e\nabla T_e + n_i\nabla T_i) = 3.3m^2/s$ is the experimental effective single fluid heat diffusivity averaged over the pellet cycle and q is the total heat flux density. It has to be noted that pellets can also modify the temperature profile due to the local cooling and this can change heat diffusivity itself. In our case the heat diffusivity changes are within $\chi_{eff} = 2.4 - 3.8m^2/s$. Finally, it is interesting to see that the value of D_D/χ_{eff} is similar to those inferred from density peaking experiments in pure deuterium plasmas [19, 20]

As mentioned previously, simulations of neutron rate could indicate that penetration of deuterium to the plasma core is faster at the beginning of pellet train compared to the later pellet fuelling phase. If enhancement of neutron rate by knock-on effect is insignificant then the value of D_D/χ_{eff} could be higher up to a factor of ~ 3 during the first pellet as seen in figure 3a from the low value of simulated neutron rate during the first pellet, even for elevated particle diffusion multiplier of $C_D = 7$. One possible interpretation is that propagation of deuterium to the core depends on the isotope mix itself. This would link our data to the previous observations of enhanced particle diffusivity in the trace tritium experiment [21] and experiments with variable H:D mix [5], though both with gas fuelling. The detailed modelling of core particle transport under mixed isotope conditions is outside the scope of this paper and will be subject of future analysis, similar to that of gas fuelled plasmas [22].

5. Conclusion

We have demonstrated control of hydrogen isotope mix in the plasma core when one isotope was delivered solely by shallow pellets from the edge. In our case we used deuterium pellets while neutral beams and gas fuelling used hydrogen. The isotope mix in the core was measured directly by charge exchange spectroscopy. In addition, the isotope mix ratio was indirectly deduced from modelling using JINTRAC code by matching the neutron rate and electron density including pellets transients. Both

methods show that the H:D isotope mix in the core reached the ratio 55:45%, close to the target. The pellet particle flux required to reach such a mix ratio is $\Phi_{pel} = 0.045 P_{aux}/T_{e,pel}$. This value is in line with conventional shallow pellet fuelling experiments using deuterium pellets and deuterium plasma. Such similarity indicates that the pellet fuelling efficiency is governed by the same particle loss mechanism regardless of isotope mix, namely the convective loss due to ELMs.

Deuterium is fuelled by edge pellets, and its particle transport is consistent with a simple model. Modelling also suggests that deuterium particle diffusivity could be higher at the beginning of the pellet train when the plasma mainly consists of hydrogen compared to flat top phase. For efficient burn control there is a demand for fast response of the isotope mix ratio to the source modifications. As shown here this could be on the order of the energy confinement time. Future work will concentrate on modelling the particle transport in the pellet cycle with more first-principle-based transport models.

Although the need for accuracy of isotope ratio control does not look very demanding it is important to understand all aspects of this control loop. In particular the question of isotope separation is important. It becomes clear that the isotope control by pellet injectors with pure isotopes is very expensive and leads to high tritium inventory with all consequences for environment. It is therefore important to build the physics basis for integrated pellet fuelling/isotope control to find the minimum isotope separation ratio which is still consistent with reliable burn control.

Acknowledgements

his work was carried out within the framework of the EUROfusion Consortium and received funding from the Euratom research and training programme 2014–2018 and 2018-2020 under grant agreement No. 633053 and from the RCUK Energy Programme grant No. EP/P012450/1. The views and opinions expressed herein do not necessarily reflect those of the European Commission.

References

- [1] Estrada-Mila C, Candy J, and R. E. Waltz R E, Phys. Plasmas 12, 022305 (2005).
- [2] Angioni C et al., Phys. Plasmas 25, 082517 (2018)
- [3] Mikkelsen D et al., Phys. Plasmas 22, 062301 (2015)
- [4] Bourdelle C et al 2018 Nucl. Fusion 58 076028
- [5] Maslov M et al Nucl. Fusion 58 (2018) 076022 <https://doi.org/10.1088/1741-4326/aac342>
- [6] Maruyama S et al 2012 Proc. 24th Int. Conf. on Fusion Energy (San Diego, 2012) ITR/P5-24 (<http://naweb.iaea.org/napc/physics/FEC/FEC2012/index.htm>)
- [7] Polevoi A et al Nucl. Fusion (2018) 58 056020 <https://doi.org/10.1088/1741-4326/aab4ad>
- [8] Day C and Giegerich T Fusion Engineering and Design 88 (2013) 616– 620
- [9] Lang P T et al Nucl. Fusion 59 (2019) 026003
- [10] Romanelli, M.; Corrigan, G.; Parail, V.; Wiesen, S.; Ambrosino, R.; da Silva Aresta Belo, P.; Garzotti, L.; Harting, D.; Koechl, F.; Koskela, T.; Lauro-Taroni, L.; Marchetto, C.; Mattei, M.; Militello Asp, E.; Nave, F.; Pamela, S.; Salmi, A.; Strand, P.; Szepesi, G. & JET EFDA contributors (2014), 'JINTRAC: A System of Codes for Integrated Simulation of Tokamak Scenarios', Plasma and Fusion Research 9, 3403023 <http://dx.doi.org/10.1585/pfr.9.3403023>
- [11] Garzotti L et al Nucl. Fusion 43 (2003) 1829–1836
- [12] Parail V et al. Nucl. Fusion 49 (2009) 075030
- [13] Köchl F et al Plasma Phys. Control. Fusion 60 (2018) 074008 <https://doi.org/10.1088/1361-6587/aabf52>
- [14] Pegourie B., Waller V., Nehme H., Garzotti L. and Geraud A. 2007 Nucl. Fusion 47 44–56
- [15] TRANSP code version 18.2, <https://transp.pppl.gov> DOI: 10.11578/dc.20180627.4
- [16] Kiptily V 2018 private communication
- [17] Valovič M et al Nucl. Fusion 56 (2016) 066009 doi:10.1088/0029-5515/56/6/066009
- [18] Valovič M et al Plasma Phys. Control. Fusion 60 (2018) 085013 <https://doi.org/10.1088/1361-6587/aacac3>
- [19] Garzotti L et al Nucl. Fusion 46 (2006) 994–1000
- [20] Valovič M et al Plasma Phys. Control. Fusion 46 (2004) 1877–1889
- [21] Zastrow K-D et al Plasma Phys. Control. Fusion 46 (2004) B255–B265
- [22] Marin M et al Nucl. Fusion to be submitted